3-D Ultrasound Guidance of Surgical Robotics: A Feasibility Study

Eric C. Pua, Matthew P. Fronheiser, Joanna R. Noble, Edward D. Light, *Member, IEEE*, Patrick D. Wolf, *Member, IEEE*, Daniel von Allmen, and Stephen W. Smith, *Member, IEEE*

***Abstract*—Laparoscopic ultrasound has seen increased use as a surgical aide in general, gynecological, and urological procedures. The application of real-time, three-dimensional (RT3D) ultrasound to these laparoscopic procedures may increase information available to the surgeon and serve as an additional intraoperative guidance tool. The integration of RT3D with recent advances in robotic surgery also can increase automation and ease of use. In this study, a 1-cm diameter probe for RT3D has been used laparoscopically for *in vivo* imaging of a canine. The probe, which operates at 5 MHz, was used to image the spleen, liver, and gall bladder as well as to guide surgical instruments. Furthermore, the three-dimensional (3-D) measurement system of the volumetric scanner used with this probe was tested as a guidance mechanism for a robotic linear motion system in order to simulate the feasibility of RT3D/robotic surgery integration. Using images acquired with the 3-D laparoscopic ultrasound device, coordinates were acquired by the scanner and used to direct a robotically controlled needle toward desired *in vitro* targets as well as targets in a post-mortem canine. The rms error for these measurements was 1.34 mm using optical alignment and 0.76 mm using ultrasound alignment.**

I. Introduction

In recent years, the development of endoscopic transducer designs has enabled the application of B-scan laparoscopic ultrasound as a preoperative and intraoperative tool for assistance in surgical guidance and assessment. The primary advantage of laparoscopic ultrasound (LUS) is the ability to image beyond tissue boundaries. Optical laparoscopes only provide views of the outer surface of organs, and laparoscopic graspers can give only a rudimentary feedback regarding tissue texture or underlying masses [1]. The integration of LUS into the operating room provides visualization of most surrounding soft tissue structures, allowing access to information that might otherwise be available only in an open surgery setting. Additionally, the ability to place the transducer directly against an organ allows the use of higher frequency devices, which provide better resolution [2].

Manuscript received March 10, 2006; accepted May 19, 2006. This research was supported by NIH grants HL 72840 and HL 64962 and NSF grant DMR313764.

E. C. Pua, M. P. Fronheiser, J. R. Noble, E. D. Light, P. D. Wolf, and S. W. Smith are with the Department of Biomedical Engineering, Duke University, Durham, NC 27705 (e-mail: ecp2@duke.edu).

D. von Allmen is with the Department of Pediatric Surgery, University of North Carolina at Chapel Hill, Chapel Hill, NC 27705.

Digital Object Identifier 10.1109/TUFFC.2006.140

Laparoscopic ultrasound has been used effectively during minimally invasive surgeries and for cancer staging in the liver and in urological applications. For cancer staging, LUS is used for tumor detection, localization and border definition, and postoperative analysis. Combined with endoscopic ultrasound, it has been used for localization of gastric submucosal tumors targeted for resection [3]. In addition to gastric and hepatic cancers, LUS also has been used as an aid for treatment of pancreatic and adrenal tumors [4], [5]. Furthermore, there has been an increase in investigations using laparoscopic ultrasound in gynecological cases, such as the treatment of uterine myomas [6], [7].

The application of real-time, three-dimensional (RT3D) ultrasound imaging may increase the use of laparoscopic ultrasound for these applications. Although acquiring full volumes of information intraoperatively, real-time, 3-D ultrasound may provide improved visualization and possibly decrease procedure time and difficulty. The ability to visualize multiple planes through a volume in real-time without moving the transducer can improve determination of target geometry as well. Acquisition of volumetric data with RT3D is achieved through the use of 2-D transducer arrays and sector-phased array scanning in both the azimuth and elevation directions [8]. In this way, pyramidal volumes of data, as shown in Fig. 1, are acquired without the use of mechanical translation or postacquisition reconstruction.

Real-time, 3-D ultrasound originally was developed at Duke University by Smith *et al.* [8] and von Ramm *et al.* [9] for cardiac imaging and commercialized by Volumetric Medical Imaging. The Duke/VMI scanner (Volumetrics Medical Imaging, Durham, NC) can display, in real-time, two orthogonal B-scans and up to three parallel C-scans at any angle and depth throughout the acquired volume, as well as RT3D rendering, 3-D color, and 3-D pulse Doppler. The original Duke prototype RT3D scanner also had the capacity of a stereoscopic display [9] to provide a better 3-D depiction of interventional devices and soft tissues. Transthoracic echocardiographic studies using RT3D have been effective for applications such as monitoring left ventricular function [10], detecting perfusion defects [11], and evaluating congenital abnormalities [12]. More recently, catheter-based transducers with 2-D arrays have been developed for intracardiac echocardiography [13]. These devices have been fabricated into 7F catheters with as many as 112 channels [14], successfully merging functional intracorporeal size with clinically relevant resolution for RT3D. Advances from the design of

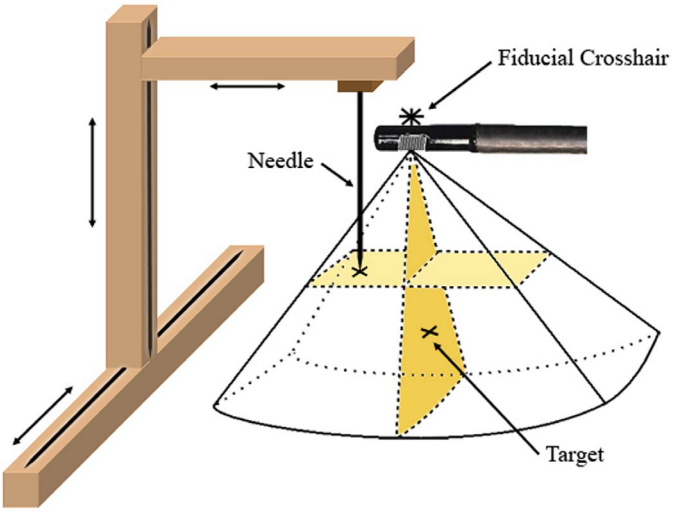

Fig. 1. Schematic of a RT3D laparoscopic probe used in conjunction with a robotic device for surgical guidance. The RT3D system can scan a pyramidal volume and display up to two B-scans (dark shade) and three parallel C-scans (light shade).

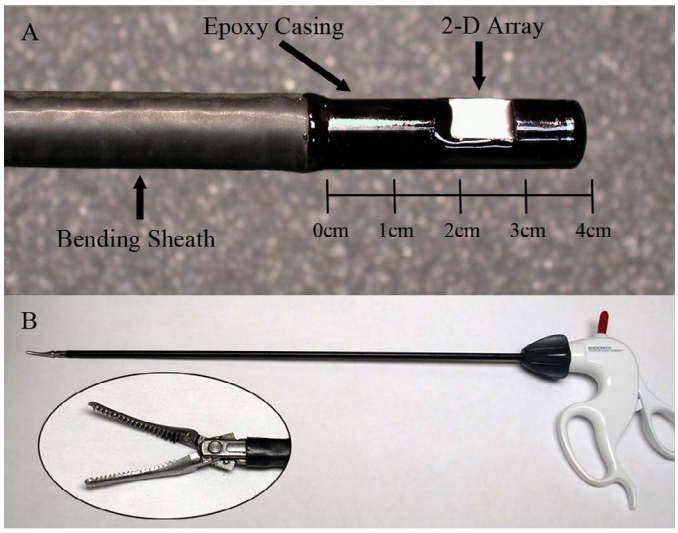

Fig. 2. Close-up of a 3-D laparoscopic probe (A) with a four-directional bending sheath and 6.3 mm × 6.3 mm aperture and (B) a 5 mm diameter Endopath surgical forceps.

intracardiac catheters have been the catalyst for the recent fabrication of endoscopic [15] and laparoscopic [16] 3-D probes we have used for cardiac applications. These have been constructed with 504 active channels at operating frequencies ranging from 5 to 7 MHz. We believe these latter devices also are well-suited for assisting in laparoscopic surgeries, serving as a preoperative tool as well as a means of intraoperative guidance.

An additional advantage that RT3D laparoscopic ultrasound provides over conventional 2-D LUS is the ability to establish a true 3-D coordinate system for measurement and guidance. Traditional ultrasound scanner systems are capable of 2-D measurements. With volumes of data acquired in real-time, RT3D scanners can provide a surgeon with 3-D structural orientation within a target organ using its measurement system, providing more information than was previously available. This could be particularly useful in conjunction with recent advancements in robotic surgeries. With new equipment such as the da Vinci robotic surgical system (Intuitive Surgical, Inc., Sunnyvale, CA), the integration of RT3D and its measurements can help locate targets and steer the robot's arms into position, while avoiding regions that must not be damaged.

Robotic surgery technology has made recent gains as an accepted alternative to traditional instruments in cardiovascular, neurological, orthopedic, urological, and general surgery. With the da Vinci system, a multicamera endoscope is used for 3-D visualization, increasing visibility and depth perception for the robot operator. The dual-lens endoscope links to two monitors, enabling 3-D stereoscopic vision within the patient. The robotic arms also exhibit precise, dexterous control, eliminating tremor and improving ergonomics for the surgeon [17]. For laparoscopic procedures, reports have been published of using robotics in cases of splenectomy, adrenalectomy, cholecystectomy, and gastric bypass among others [18]–[20]. In most cases, surgeons reported better visualization, increased instrument control, reduced operator fatigue, and an improved learning curve for those training to perform these procedures [17], [21].

In this paper, we demonstrate the use of RT3D ultrasound in a laparoscopic setting and its feasibility as a direct guidance tool for robotic surgery. A steerable RT3D probe [Fig. 2(A)] has been modified for use as a laparoscope and used for *in vivo* imaging of a canine model. During a minimally invasive procedure, this probe was used to produce volumetric scans of the liver, spleen, and gall bladder and to introduce hypoechoic targets.

In addition, the probe was used *in vitro* in conjunction with the Volumetrics measurement system and a robotic linear motion system to demonstrate the feasibility of the use of RT3D for semiautomated guidance of a surgical robot. A simplified schematic of the two systems working in concert is shown in Fig. 1. The combination of RT3D and robotics for laparoscopic surgery may improve procedure accuracy and decrease operation time and difficulty. Integration of the two systems also can increase automation in cases such as biopsies and allow for the establishment of regions in which the robotic instruments must not operate.

II. Materials and Methods

A. Volumetrics Scanner System and 3-D Laparoscopic Probe

The Duke/Volumetrics 3-D scanner system that implements RT3D uses up to 512 transmitters and 256 receivers with 16:1 receive mode parallel processing. The system is capable of acquiring 4100 B-mode image lines at a rate of

TABLE I
DOCUMENTED MEASUREMENT ERROR OF VOLUMETRICS SYSTEM.

Scan type	Target depths	% Error
B-Scan	3–12 cm	2.31
C-Scan	3–12 cm	5.5

up to 30 volumes per second with scan angles from 60 to 120 degrees. This acquisition produces a pyramidal volume equivalent to 64 sector scans of 64 lines each, stacked in the elevation dimension. The system's display scheme permits the simultaneous visualization of two standard orthogonal B-scans as well as up to three C-scan planes parallel to the face of the transducer array. The B-scans and C-scans can be tilted at any angle, and the angle and depth of the C-scans can be changed in real-time. Integration and spatial filtering of the data encompassed by two C-scan planes provides a real-time, volume-rendered image.

A real-time scan converter transforms echo data from the 3-D spherical (r, θ, φ) geometry of the pyramidal scan to the rectangular (x, y, z) geometry of the television display. The xyz coordinates provided by the measuring program for distance, area, and volume calculations are derived from scan converter viewport tables that generate the image slices for the display. These viewport tables, in turn, are assembled from a 3-D, cubic decimation/interpolation system on the scan conversion field-programmable gate array (FPGA) chips, which accept the depth, azimuth angle, and elevation angle from the received echo data and convert them to rectangular coordinates. The original, documented measurement error of the Volumetrics system is shown in Table I[1]. These values reflect the average length error in measurements made in the designated scan type over the given range of depth. Variability over this target range is provided by the manufacturer.

The transducer used for all the described experiments is a 504 channel matrix array probe originally designed for transesophageal echocardiography (TEE) [15], as shown in Fig. 2(A). A 4-directional bending sheath is incorporated into the tip of the probe. This steering function also provides quick orientation adjustment in any direction. The 3-D TEE probe operates at 5 MHz using a 6.3 mm × 6.3 mm aperture. Its outer diameter at the probe tip is 1 cm.

B. Animal Model and 3-D Laparoscopic Study

The Institutional Animal Care and Use Committee approved the use of a canine model for the acquisition of *in vivo*, 3-D images, conforming to the Research Animal Use Guidelines of the American Heart Association. Ketamine hydrochloride 10–15 mg/kg was injected intramuscularly to sedate the dog. An intravenous solution of 0.9% sodium chloride was established in the peripheral vein and maintained at 5 mL/kg/minute. Anesthesia was induced via nasal inhalation of isoflurane gas 1–5%. An endotracheal tube for artificial respiration was inserted after oral intubation with the dog placed on its back on a water-heated thermal pad. A femoral arterial line was placed on the left side via a percutaneous puncture. Electrolyte and respirator adjustments were made based on serial electrolyte and arterial blood gas measurements. Blood pressure, electrocardiogram, and temperature were continuously monitored throughout the procedure.

After the animal preparations were complete, the dog's abdominal cavity was insufflated with carbon dioxide gas. Four surgical trocar ports were introduced into this cavity. One port was designated for an optical laparoscope. Two others were used primarily for surgical forceps and introducing imaging targets. The 3-D laparoscopic ultrasound probe was introduced into the fourth port with its bending sheath flexed to 90 degrees in order to facilitate contact with the canine's organs. The probe was guided to the desired locations using the optical laparoscope. Once all instruments were in place, images of the spleen, liver, and gall bladder were acquired before and after introduction of forceps. In addition, an XXL™ balloon dilatation catheter (Boston Scientific, Watertown, MA) was introduced into the liver and the spleen to provide a hypoechoic imaging target for the 3-D probe to locate. The catheter is a 5.8 Fr device with an inflated balloon size of 12 mm by 2 cm. All imaging and surgical procedures were monitored via the optical laparoscope.

C. Feasibility of RT3D Measurement for Robotic Guidance

The robot used for these feasibility experiments was a Gantry III Cartesian Robot Linear Motion System manufactured by Techno-Isel (Techno, Inc., New Hyde Park, NY). A simplified representation of this device is shown in Fig. 1. It uses a Model H26T55-MAC200SD automated controller that accepts input commands and 3-D coordinates from a connected computer. The XY stage (model HL32SBM201201505) is a stepper motor design providing 340 mm × 290 mm of travel on a 600 mm × 500 mm stage. The Z-axis slide (model HL31SBM23051005) provides 125 mm of vertical clearance and allows 80 mm of travel in the z-dimension.

An accuracy profile of the Volumetrics measurement system in coordination with a robotic device was acquired. Three different measurement targets were used for accuracy measurements. The B-scan target consisted of 19 wire targets in a water tank spaced 7 mm apart with an 8 cm radius of curvature. The 3-D scan target was constructed of two rows of seven vertically oriented wire targets spaced 5 mm apart. The two rows were separated by 15 mm. The third phantom used for the experiment was a 3-cm diameter, hypoechoic lesion inside a tissue-mimicking slurry [22].

For these measurements, the aforementioned 3-D laparoscopic probe, connected to the Volumetrics scanner, was flexed at the bending sheath 90 degrees in the elevation plane in order to face downward into a water tank or tissue-mimicking medium, located on the XY stage of the

[1]Volumetrics Medical Imaging, *Guide to the Model 1 Scanner*, Durham, NC, pp. C5–C6, 1998.

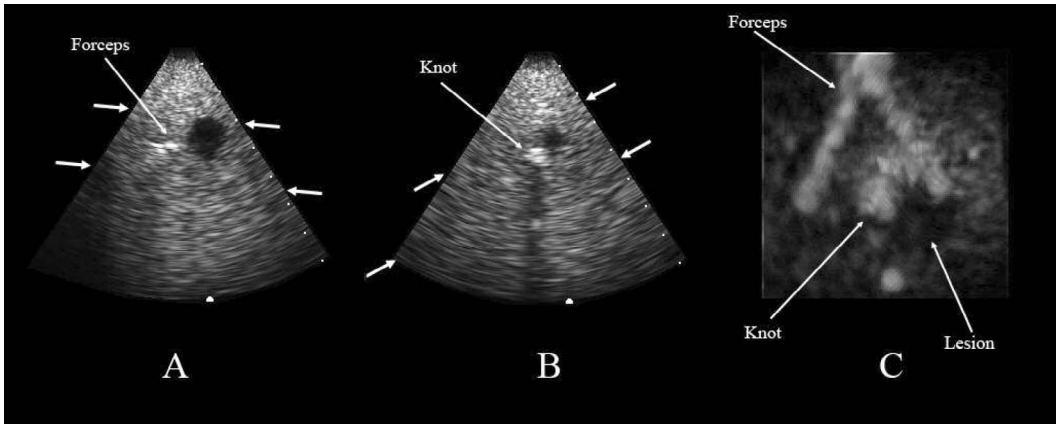

Fig. 3. Images of a 12 mm hypoechoic lesion in a tissue-mimicking medium. The elevation (A) and azimuth (B) B-scans show the lesion. An out-of-plane pair of surgical forceps [Fig. 2(B)] is visible in the volume-rendered view (C).

Cartesian robot. A fiducial crosshair, illustrated in Fig. 1, was etched into the back of the 3-D probe for optical alignment of a robotically guided, 1.2-mm diameter needle with the center of the transducer face. Once the transesophageal (TE) probe transducer face was aligned to provide a view of the desired measurement targets on the scanner, the needle was centered on the back of the transducer using the robot controller. The Volumetrics scanner then was used to image the target. Once frozen, target coordinates were taken using the scanner measurement system. With the robot's frame of reference zeroed on the transducer's fiducial spot, these coordinates were input into the robot controller, allowing for the 1-cm thickness of the probe. Once the robot had positioned the needle according to the coordinates predicted by the 3-D image, the tip was repositioned via the robot's stepping function in 0.1-mm increments in 3-D until it made contact with the target. Visual confirmation of contact was used to determine whether repositioning was complete. The adjusted coordinates from the robot controller were recorded in order to calculate rms error. A series of 10 measurements was taken for the B-scan target phantom, and 16 data points were collected for the 3-D scan targets. This data was collected over several trials; the phantom and transducer setup was dismantled at the end of each experiment.

An additional 12 measurements were taken in the 3-D scanning mode for ultrasound alignment without centering the needle on the fiducial crosshair. In this setup, the transducer was flexed in the opposite direction and placed at the bottom of the water tank, facing upward. The guided needle was lowered until it was visible at an arbitrary location in one of the B-scan or C-scan displays. The other B-scan slice was selected to show one of the 3-D scan targets. Coordinates for the tip of the needle (x, y, z) and the desired target (x', y', z') were acquired using each B-scan or a C-scan plane, and the differences ($\Delta x = x - x'$, $\Delta y = y - y'$, $\Delta z = z - z'$) were calculated. The needle then was moved by Δx, Δy, Δz relative to its original location in order to make contact with the 3-D scan target. The rms error measurements were recorded using 0.1-mm increments, as stated before.

In a third experiment, the optical alignment method was used for guiding a needle toward a designated target on the organ boundaries in a postmortem canine. For this study, a fresh canine cadaver was placed on the XY stage of the robot, and an approximately 30-cm long incision was made to open the abdomen, starting at the base of the sternum. The RT3D probe was flexed into the downward facing position, and the array face was placed in contact with the liver and gall bladder. Optical alignment was used for centering the tip of a 1.2-mm diameter, 15-cm long needle on the fiducial crosshair. The VMI scanner was used to determine the distance for the needle to travel in order to puncture the distal boundary of the gall bladder at a desired location. Visualization of the needle movement was recorded with a digital camera simultaneously with the RT3D scans using a video screen-splitting device.

III. Results

A. Images

Real-time images of *in vivo* canine anatomy and robotic surgical targeting were acquired with the Model V360 and Model 1 Volumetrics scanners interfaced with the described 3-D laparoscopic probe. These images (Figs. 4–10) include user-selected, 60 degree and 90 degree B-scans, C-scans, and 3-D volume-rendered scans. The intersections of multiple B-scan planes are indicated by blunt arrowheads at the base of elevation and azimuth scans; larger arrows to the sides indicate the planes used for each C-scan or volume-rendered image. The depth scale of each scan is shown by the white dots along the sides of each B-scan, each dot indicating 1 cm. The scale of the 3-D rendered images does not directly correspond with that of the corresponding B-scans.

In Fig. 3, the *in vitro* image quality and volume rendering capabilities of the 3-D laparoscopic probe are shown. The image was taken from an 8-cm deep, 60 degree, 3-D scan of a tissue-mimicking slurry with a 12-mm hypoechoic lesion (water balloon) suspended in the medium.

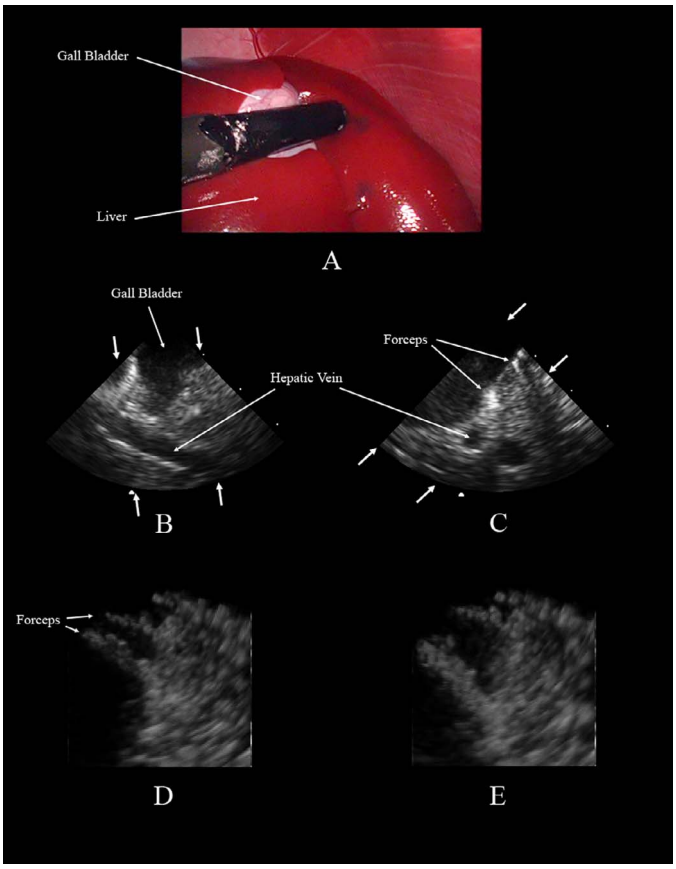

Fig. 4. Simultaneous optical laparoscopic view (A) and 3-D laparoscopic ultrasound of the liver and gall bladder. The azimuth (B) and elevation (C) B-scans show the hypoechoic gall bladder and hepatic vein. A pair of surgical forceps [Fig. 2(B)] located between the two organs is visible in the volume-rendered view in both a closed (D) and opened position (E).

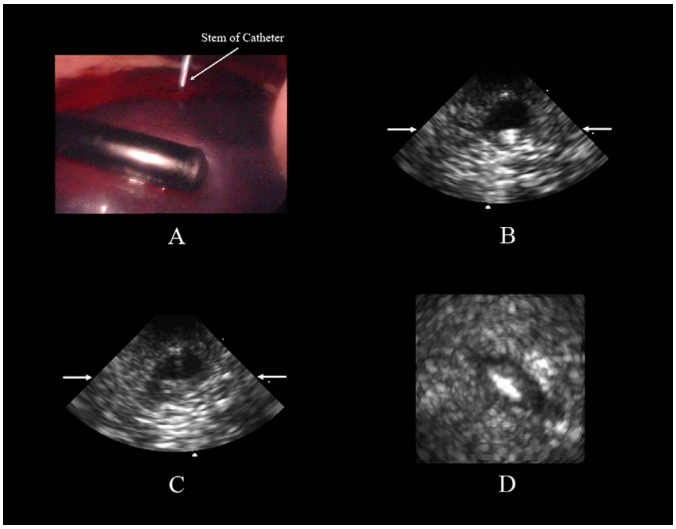

Fig. 5. Simultaneous optical laparoscope view (A) and 3-D laparoscopic ultrasound of the spleen. A hypoechoic imaging target introduced in the spleen is seen in short axis cross section in the B-scans (B and C). The long-axis profile with the central spine of the target is visible in the C-scan (D).

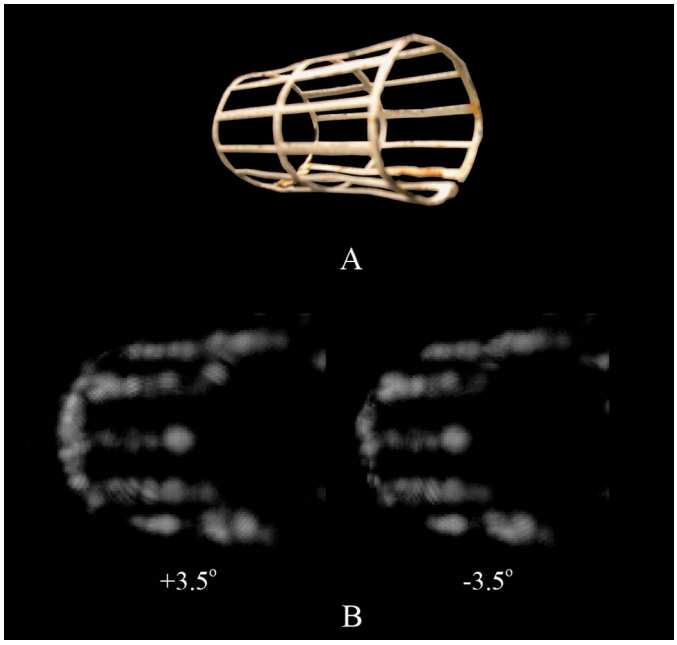

Fig. 6. 3-D stereoscopic imaging with RT3D ultrasound. The cylindrical metal cage (A) is 4.4 cm in diameter and 8.9 cm in length. The 3-D image is constructed by fusing the volume-rendered left-eye (+3.5°) and right-eye (−3.5°) views (B).

The elevation B-scan [Fig. 3(A)] shows the full diameter of the lesion. Barely visible in this view is the stem of a 5-mm Endopath surgical forceps instrument (Ethicon Endo-Surgery, Cincinatti, OH) [Fig. 2(B)]. The azimuth B-scan [Fig. 3(B)] shows a portion of the lesion and the knot from which it is anchored. The knot of the target produces shadowing throughout the rest of the scan. The forceps are clearly visible only in the volume-rendered view [Fig. 3(C)], which has been acquired using the data between the planes indicated by the arrows. In this image, the open forceps are rendered in the foreground with the lesion and its point of attachment in the background.

Fig. 4 shows a 4-cm deep, 90 degree scan of the gall bladder. In Fig. 4(A), the transducer face is placed against the gall bladder with liver tissue surrounding it. A short axis [Fig. 4(B)] and long axis [Fig. 4(C)] view of the gall bladder are both visible in the displayed B-scans. Also visible in these B-scans are a long axis [Fig. 4(B)] and short axis [Fig. 4(C)] view of the hepatic vein, approximately 5-mm in diameter. Not shown in the optical view, surgical forceps [Fig. 2(B)] are present between the surfaces of the gall bladder and the liver of the canine. The jaws of the forceps can be seen both partially closed and opened in the volume-rendered images [Fig. 4(D) and (E)]. The renderings were acquired using the ultrasound data between the C-scan planes indicated by the arrows. Close inspection of the B-scans shows cross-sectional views of the two points of the forceps in Fig. 4(C). The views of the forceps in Figs. 3 and 4 demonstrate the value of RT3D rendering over the selected slices from a 3-D scan.

For imaging the spleen, a balloon dilatation catheter was inserted to serve as a hypoechoic structure. The trans-

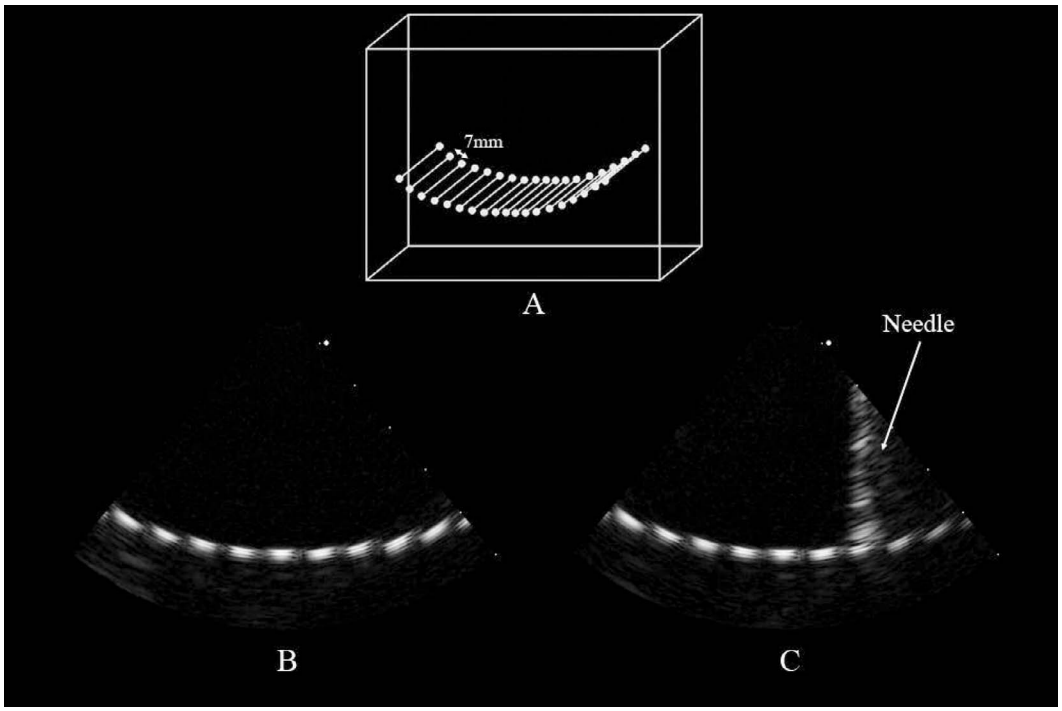

Fig. 7. Ultrasound guidance of a robotically controlled 1.3 mm needle using B-scan image measurements. The targets are spaced 7 mm apart with an 8 cm radius of curvature (A). The image used for target location is the scan of (B). (C) Shows the robot guiding the needle into position using the scanner's coordinates.

ducer placement over the spleen can be seen in Fig. 5(A), with the stem of the balloon catheter located approximately 2 cm superior to the probe. Orthogonal short axis, cross-sectional views of the inflated balloon are shown in the B-scan slices [Fig. 5(B) and (C)], using a 4-cm deep, 90 degree scan. The profile of the hypoechoic target is shown in the C-scan [Fig. 5(D)]. The bright target at the center of the balloon is the central spine of the catheter device from which the outer layer inflates.

Fig. 6 shows a real-time stereoscopic display for the 3-D scanner. The imaging target shown in Fig. 6(A) is a cylindrical metal cage 4.4 cm in diameter and 8.9 cm in length. A 65 degree, 3-D scan was used to image down the length of the target, and volume rendering planes were set to display the foremost half of the cylinder. Once the scan was acquired, separate left-eye ($+3.5°$) and right-eye ($-3.5°$) views of the volume-rendered target are shown simultaneously on the screen, as shown in Fig. 6(B). These two views can be fused by the observer as a stereoscopic pair, allowing for a 3-D visualization of the target analogous to the dual-camera system used in the da Vinci robot system.

B. Robotic Guidance Accuracy

Fig. 7 shows the B-scan phantom with a 6-cm deep, 90 degree, single B-scan. In Fig. 7(B), nine wires are clearly visible in cross section. In Fig. 7(C), the third wire from the right is in contact with the robot-controlled needle probe. For the single B-scan mode of the scanner, the rms guidance error from measurements was found to be 0.86 mm $\pm$ 0.51 mm using optical alignment. Similarly, in Fig. 8(B), orthogonal B-scans and a C-scan of the 3-D phantom are shown before the needle has been positioned. These images were attained with a 6-cm deep, 60 degree, 3-D scan. An entire row is visible in the elevation B-scan, and a pair of targets from the two rows is shown in the azimuth B-scan. The C-scan shows the profile of the 3-D phantom with all the target tips clearly visible. In Fig. 8(C), the Cartesian robot has positioned the needle to come into contact with a target in the left column, as visible in all three image planes of the scan. The mean rms error for these 3-D scan measurements was found to be 1.34 mm $\pm$ 0.68 mm using optical alignment.

A third set of measurements was taken without the use of the optical fiducial mark, using only ultrasound alignment. These yielded a mean rms error of 0.76 mm $\pm$ 0.45 mm.

For the tissue-mimicking phantom, we performed several trials at making contact with the hypoechoic lesion using both C-scan and B-scan coordinates. In Fig. 9(A), the needle has not yet been positioned with the robot, and the lesion is clearly visible in both B-scans and the accompanying C-scan. In Fig. 9(B), it is evident that the needle has come into contact with the target. The needle tip appears to be deforming the lesion slightly, as it is visible within the diameter of the target in both B-scans and in the C-scan plane. Error measurements of the needle strike point compared to the measurement point on the scanner were not taken due to the optical opacity of the graphite slurry containing the lesion; however, scan plane markers were used to identify the desired position of needle placement. These markers give an approximation of the measurement error for the experiment.

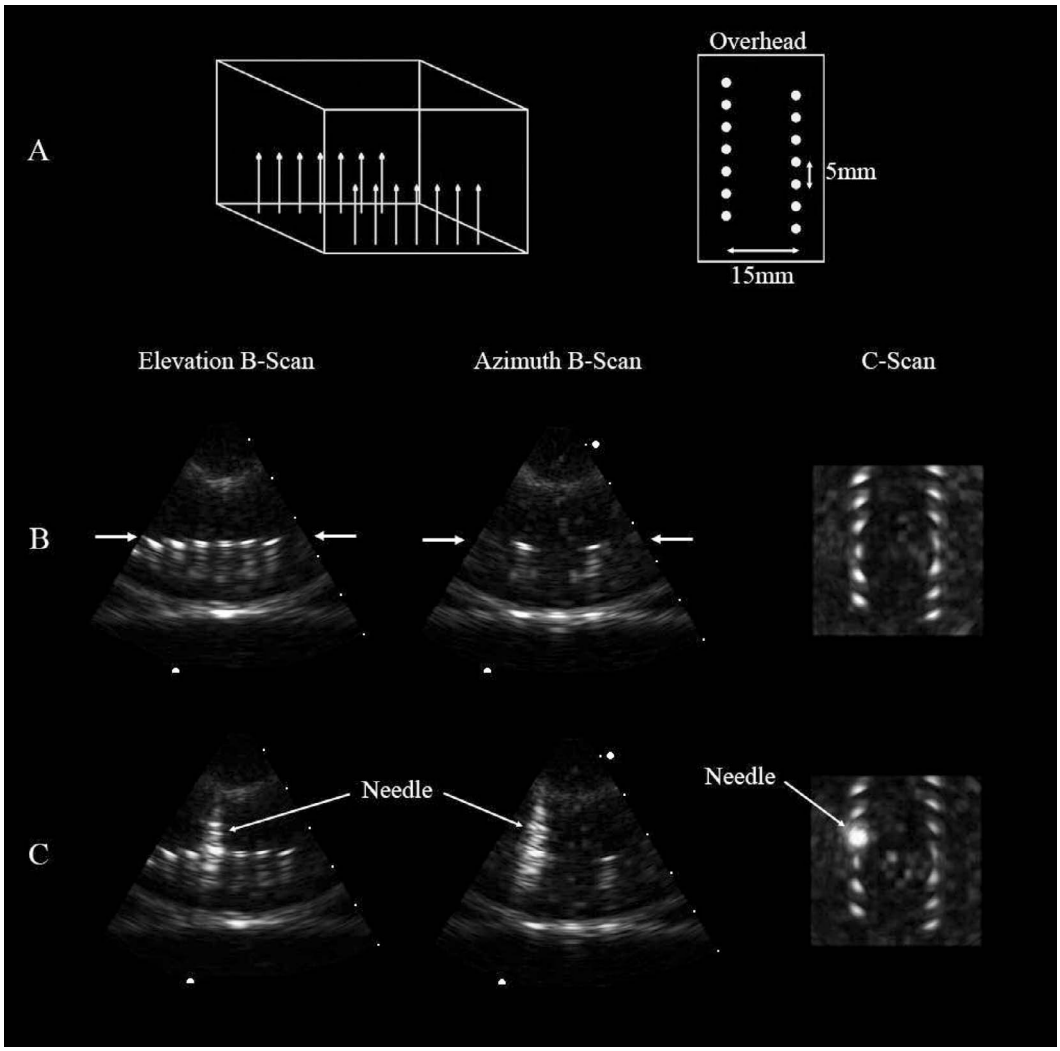

Fig. 8. 3-D ultrasound guidance of a robotically controlled 1.3 mm needle using C-scan measurements. A 3-D and overhead diagram of the 3-D scan target is shown in (A). The B-scans and C-scans used to view and locate the target are shown in the images of (B). The needle is shown in three views striking the point of the desired target in (C).

In the cadaver experiment, the coordination of the robotic motion system and 3-D ultrasound measurements were used to puncture a desired position on the distal wall of the gall bladder. The movie of Fig. 10 demonstrates the procedure. First, coordinates were acquired at the desired location in the gall bladder, indicated by the white circles in the movie. These were monitored using the green and blue scan plane markers of the azimuth and elevation B-scans. The needle can be seen in the left view as it is lowered into the cadaver's abdomen. Meanwhile, in the right view, it is clearly reaching the designated target in both B-scans. There is a small error in the azimuth B-scan that appears to be on the order of 1–2 mm.

IV. Discussion and Summary

A. 3-D Ultrasound Laparoscopy

Using a 3-D laparoscopic ultrasound probe, images of *in vivo* canine abdominal anatomy have been acquired. These scans [Figs. 4 and 5] show the image quality indicative of current prototype endoscopic probes designed for RT3D ultrasound. From these pictures, we believe that such devices are well suited for assisting in laparoscopic surgeries. In Fig. 4, volume-rendered views provide visualization of surgical instruments that were not immediately noticeable in standard B-scans. Similarly, in Fig. 5, the combination of standard B-scans with parallel C-scan views enables better spatial familiarity with the shape and size of the angioplasty balloon introduced into the spleen. In this set of images, the width, length, and interior structure of the target are all apparent simultaneously from the three displayed slices. The ability to view the acquired volumetric data stereoscopically can further enhance 3-D visualization of surgical instruments and the target region. These factors are encouraging for the application of RT3D to the laparoscopic surgery setting.

Some current limitations with this technology are size, maneuverability, and the need for higher frequency operation. For these studies, the articulation of the bending sheath was essential for maneuvering the side-scanning RT3D probe into position, particularly for the *in vivo*

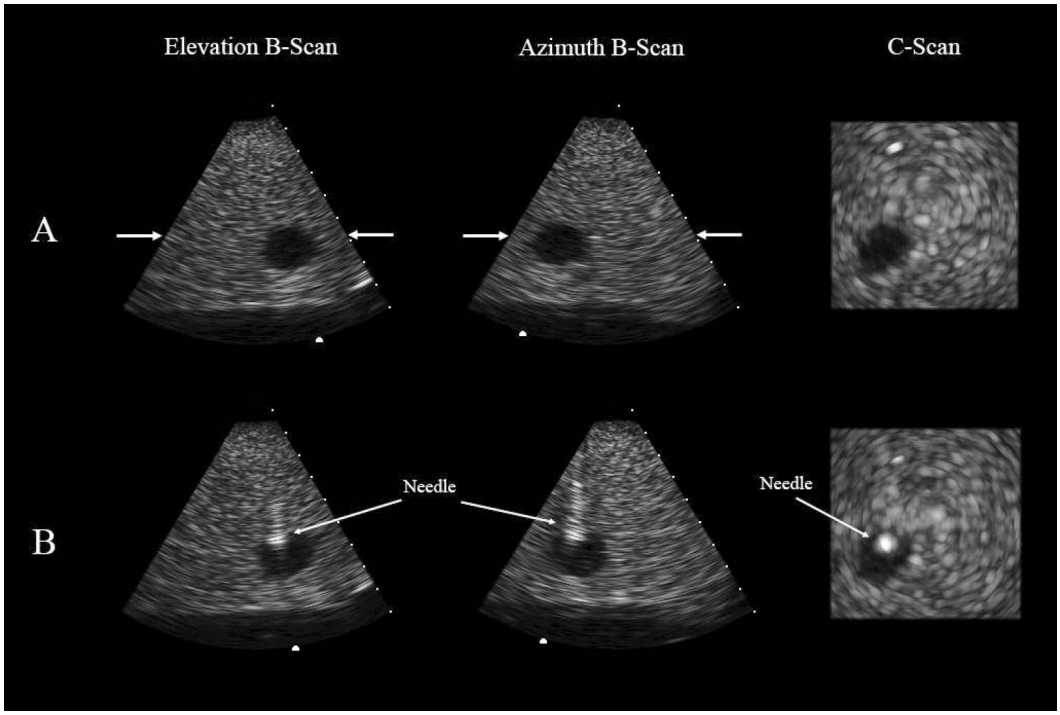

Fig. 9. Integrated 3-D ultrasound guidance and robotics for a hypoechoic lesion in a tissue-mimicking medium. The lesion's coordinates are measured from the B-scans and C-scan in (A). In (B), the needle is coming into contact with the lesion.

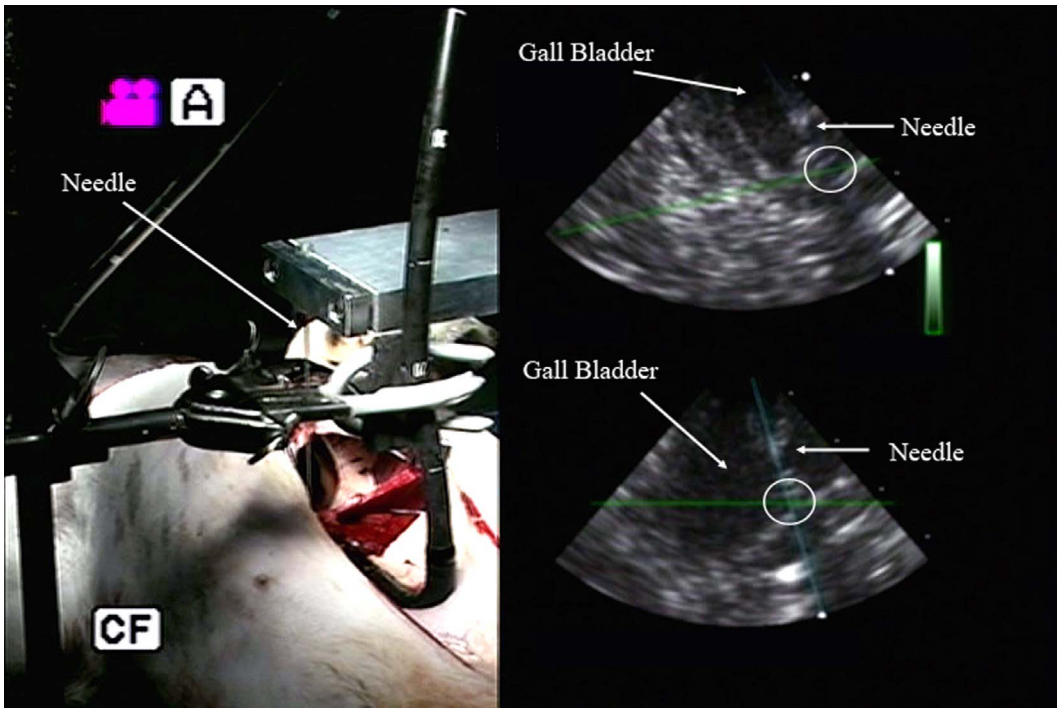

Fig. 10. Split-screen video capture of a 15-cm needle puncturing the gall bladder of a canine cadaver. The intersection of the green and blue scan plane markers indicate the desired target of the needle, which is shown in both azimuth and elevation B-scans.

imaging. However, forward-looking, 2-D array devices may be better suited for these situations if a steering mechanism were incorporated. We have developed forward-looking laparoscopic devices for RT3D with an overall diameter less than 1 cm; however, at present, we have not integrated steering abilities into these probes [16]. Also, one would ideally like to have a higher level of resolution close to the transducer face because most targets will be within the first few centimeters for a laparoscopic procedure. The image quality in this region can be improved with the use of a higher frequency, broader bandwidth probe, which could enable the addition of multifrequency operation. However, at present, 3-D laparoscopic probes have not been fabricated at operating frequencies greater than 10 MHz due to hardware limitations of the VMI scanner.

B. Robotic Guidance

Preliminary studies integrating 3-D ultrasound with a robotic device also have shown promise. The error when using the Volumetrics scanner 3-D coordinates to guide a robotic linear motion system to a specified target is less than 2 mm. A possible reason for the discrepancy in errors between the measurement methods is the elimination of user error in the case of ultrasound alignment. In the case of optical alignment, centering of the needle on the fiducial crosshair is dependent on user subjectivity. The system used for this study is capable of only three degrees of freedom; so further tests with more sophisticated robotic equipment will be necessary to prove efficacy and accuracy. However, the ability to integrate the RT3D system with robot surgical units has much potential. The last set of measurements using only ultrasound metrics is even more encouraging because optical alignment of the robotically guided device and the imaging probe is not necessary. With a margin of error of approximately 1 mm, this means that catheters and endoscopes could image the target organ from outside the surgical field, thus improving flexibility for surgical procedures. The combination of RT3D with robotic surgery systems could prove valuable when staging transcutaneous or laparoscopic biopsies or for other surgeries when defining regions of the anatomy that the robot's instruments must automatically avoid. Current efforts in this area are focused on improved integration of the two systems and on implementation for *in vivo* animal studies.

Acknowledgments

The authors would like to thank Ellen Dixon-Tulloch for her assistance during the *in vivo* animal study.

References

[1] E. Berber and A. E. Siperstein, "Laparoscopic ultrasound," *Surg. Clin. North Amer.*, vol. 84, pp. 1061–1084, 2004.

[2] R. Kolecki and B. Schirmer, "Intraoperative and laparoscopic ultrasound," *Surg. Clin. North Amer.*, vol. 78, pp. 251–271, 1998.

[3] W. J. Hyung, J. S. Lim, J. H. Cheong, Y. C. Lee, and S. H. Noh, "Tumor localization using laparoscopic ultrasound for a small submucosal tumor," *J. Surg. Oncol.*, vol. 86, pp. 164–166, 2004.

[4] S. E. Pautler, P. L. Choyke, C. P. Pavlovich, K. Daryanani, and M. M. Walther, "Intraoperative ultrasound aids in dissection during laparoscopic partial adrenalectomy," *J. Urol.*, vol. 168, pp. 1352–1355, 2002.

[5] B. N. Thomson, R. W. Parks, D. N. Redhead, F. K. Welsh, K. K. Madhavan, S. J. Wigmore, and O. J. Garden, "Refining the role of laparoscopy and laparoscopic ultrasound in the staging of presumed pancreatic head and ampullary tumours," *Br. J. Cancer*, vol. 94, pp. 213–217, 2006.

[6] C. Exacoustos, E. Zupi, D. Marconi, M. E. Romanini, B. Szabolcs, A. Piredda, and D. Arduini, "Ultrasound-assisted laparoscopic cryomyolysis: Two- and three-dimensional findings before, during and after treatment," *Ultrasound Obst. Gynec.*, vol. 25, pp. 393–400, 2005.

[7] P. C. Lin, A. Thyer, and M. R. Soules, "Intraoperative ultrasound during a laparoscopic myomectomy," *Fertil. Steril.*, vol. 81, pp. 1671–1674, 2004.

[8] S. W. Smith, H. G. Pavy, and O. T. von Ramm, "High-speed ultrasound volumetric imaging system. Part I: Transducer design and beam steering," *IEEE Trans. Ultrason., Ferroelect., Freq. Contr.*, vol. 38, pp. 100–108, 1991.

[9] O. T. von Ramm, S. W. Smith, and H. G. Pavy, "High-speed ultrasound volumetric imaging system. Part II: Parallel processing and image display," *IEEE Trans. Ultrason., Ferroelect., Freq. Contr.*, vol. 38, pp. 109–115, 1991.

[10] M. A. Schmidt, C. J. Ohazama, K. O. Agyeman, R. Z. Freidlin, M. Jones, J. M. Laurienzo, C. L. Brenneman, A. E. Arai, O. T. von Ramm, and J. A. Panza, "Real-time three-dimensional echocardiography for measurement of left ventricular volumes," *Amer. J. Cardiol.*, vol. 84, pp. 1434–1439, 1999.

[11] G. Camarano, M. Jones, R. Z. Freidlin, and J. A. Panza, "Quantitative assessment of left ventricular perfusion defects using real-time three-dimensional myocardial contrast echocardiography," *J. Amer. Soc. Echocardiogr.*, vol. 15, pp. 206–213, 2002.

[12] C. E. Fleishman, J. Li, T. Ota, C. J. Ohazama, G. Stetten, D. Adams, O. T. von Ramm, and J. Kisslo, "Identification of congenital heart defects using real time three-dimensional echo in pediatric patients," *Circulation*, vol. 94, pp. 2423–2423, 1996.

[13] E. D. Light, S. F. Idriss, P. D. Wolf, and S. W. Smith, "Real-time three-dimensional intracardiac echocardiography," *Ultrasound Med. Biol.*, vol. 27, pp. 1177–1183, 2001.

[14] W. Lee, S. F. Idriss, P. D. Wolf, and S. W. Smith, "A miniaturized catheter 2-D array for real-time, 3-D intracardiac echo cardiography," *IEEE Trans. Ultrason., Ferroelect., Freq. Contr.*, vol. 51, pp. 1334–1346, 2004.

[15] E. C. Pua, S. F. Idriss, P. D. Wolf, and S. W. Smith, "Real-time 3D transesophageal echocardiography," *Ultrason. Imag.*, vol. 26, pp. 217–232, 2004.

[16] E. D. Light, S. F. Idriss, K. F. Sullivan, P. D. Wolf, and S. W. Smith, "Real-time 3D ultrasonic laparoscopy," *Ultrason. Imag.*, vol. 27, pp. 89–100, 2005.

[17] B. P. Jacob and M. Gagner, "Robotics and general surgery," *Surg. Clin. North Amer.*, vol. 83, pp. 1405–1419, 2003.

[18] W. H. Chapman, III, R. J. Albrecht, V. B. Kim, J. A. Young, and W. R. Chitwood, Jr., "Computer-assisted laparoscopic splenectomy with the da Vinci surgical robot," *J. Laparoendoscopic Adv. Surg. Techniques*, vol. 12, pp. 155–159, 2002.

[19] F. Corcione, C. Esposito, D. Cuccurullo, A. Settembre, N. Miranda, F. Amato, F. Pirozzi, and P. Caiazzo, "Advantages and limits of robot-assisted laparoscopic surgery: Preliminary experience," *Surg. Endoscopy*, vol. 19, pp. 117–119, 2005.

[20] G. A. Khairy, M. Fouda, A. Abdulkarim, A. Al-Saigh, and K. Al-Kattan, "A new era in laparoscopic surgery. Evaluation of robot-assisted laparoscopic procedures," *Saudi Med. J.*, vol. 26, pp. 777–780, 2005.

[21] G. Hubens, H. Coveliers, L. Balliu, M. Ruppert, and W. Vaneerdeweg, "A performance study comparing manual and robotically assisted laparoscopic surgery using the da Vinci system," *Surg. Endoscopy*, vol. 17, pp. 1595–1599, 2003.

[22] E. L. Madsen, J. A. Zagzebski, M. F. Insana, T. M. Burke, and G. Frank, "Ultrasonically tissue-mimicking liver including the frequency dependence of backscatter," *Med. Phys.*, vol. 9, pp. 703–710, 1982.

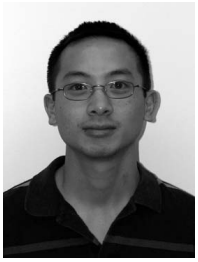

Eric C. Pua was born in Chattanooga, TN on June 29, 1979. He received a B.S.E. degree in Biomedical Engineering in 2001 from Duke University, Durham, NC.

Currently, he is a doctoral candidate in the Biomedical Engineering department at Duke University. His research focuses on the development of endoscopic devices for real-time 3-D ultrasound imaging and therapy.

Matthew P. Fronheiser was born in Pottstown, PA, on January 13, 1980. He received a B.S. degree in biomedical engineering from the Catholic University of America, Washington, DC, in 2002.

Currently, he is a biomedical engineering doctoral candidate at Duke University, Durham, NC. His current research focuses on the guidance of interventional devices during minimally invasive surgery using real-time volumetric imaging.

Joanna Noble was born in Tulsa, OK, on June 6, 1985. She is a biomedical engineering undergraduate at Duke University, Durham, NC. Her research focuses on stereoscopic 3-D display of ultrasound data.

Edward D. Light (M'00) was born in Charlottesville, VA, in 1967. He received a B.S.E. degree in Biomedical Engineering and an M.S. in Biomedical Engineering in 1989 and 1997, respectively, both from Duke University, Durham, NC.

Since 1989 he has worked as an R&D Engineer at Duke developing 2-D arrays for real time volumetric imaging. He holds several patents in the field of catheter based ultrasound imaging. He is currently pursuing his research interests in novel applications of 2-D arrays to the areas of catheter based and endoscopic based ultrasound imaging.

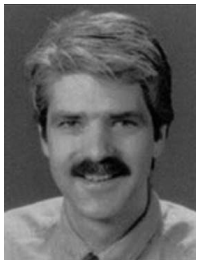

Patrick D. Wolf (M'89) was born in Altoona, PA, in 1956. He received a B.S. degree in electrical engineering and an M.S. degree in bioengineering from the Pennsylvania State University, State College, PA. After receiving his Ph.D. degree from Duke University, Durham, NC, in 1992, he joined the faculty in biomedical engineering and is currently pursuing his research interests in instrumentation, cardiac arrhythmias, and the brain-machine interface.

Daniel von Allmen is an Associate Professor of Surgery at the University of North Carolina. He received his undergraduate degree from Williams College in 1980 and his medical degree from the University of Vermont in 1986. He trained in general surgery at the University of Cincinnati and in pediatric surgery at the Children's Hospital Medical Center in Cincinnati. He has held faculty positions at the University of Pennsylvania and UNC.

Dr. von Allmen is currently chief of the Division of Pediatric Surgery at UNC and is the Surgeon-in-Chief of the North Carolina Children's Hospital. His clinical interests are in the surgical treatment of pediatric inflammatory bowel disease, surgical oncology, and the use of minimally invasive surgical techniques. His research interests are in the development of advanced surgical technologies and surgical robotics.

Stephen W. Smith (M'91) was born in Covington, KY, on July 27, 1947. He received the B.A. degree in physics (summa cum laude) in 1967 from Thomas More College, Ft. Mitchell, KY, the M.S. degree in physics in 1969 from Iowa State University, Ames, and the Ph.D. degree in biomedical engineering in 1975 from Duke University, Durham, NC.

In 1969, he became a Commissioned Officer in the U.S. Public Health Service, assigned to the Food and Drug Administration, Center for Devices and Radiological Health, Rockville, MD, where he worked until 1990 in the study of medical imaging, particularly diagnostic ultrasound and in the development of performance standards for such equipment. In 1978, he became an adjunct associate professor of radiology at Duke University Medical Center. In 1990, he became an associate professor of biomedical engineering and radiology, and Director of Undergraduate Studies in Biomedical Engineering at Duke University. He holds 16 patents in medical ultrasound and has authored 100+ publications in the field.

Dr. Smith is cofounder of Volumetrics Medical Imaging. He has served on the education committee of the American Institute of Ultrasound in Medicine, the executive board of the American Registry of Diagnostic Medical Sonographers, the editorial board of *Ultrasonic Imaging*, and the Technical Program Committee of IEEE-UFFC. He was corecipient of the American Institute of Ultrasound in Medicine Matzuk Award in 1988 and 1990 and corecipient of the IEEE-UFFC Outstanding Paper Award in 1983 and 1994.